frontiers | Frontiers in Physics

TYPE Original Research
PUBLISHED 11 July 2023
DOI 10.3389/fphy.2023.1211166

OPEN ACCESS

EDITED BY
Chunqi Jiang,
Old Dominion University, United States

REVIEWED BY
Nikola Skoro,
University of Belgrade, Serbia
Eric ROBERT,
UMR7344 Groupe de recherches sur l'énergétique des milieux ionisés (GREMI), France

*CORRESPONDENCE
Pankaj Attri,
chem.pankaj@gmail.com

RECEIVED 24 April 2023
ACCEPTED 28 June 2023
PUBLISHED 11 July 2023

CITATION
Attri P, Okumura T, Takeuchi N, Kamataki K, Koga K and Shiratani M (2023), Plasma-assisted CO_2 and N_2 conversion to plant nutrient.
Front. Phys. 11:1211166.
doi: 10.3389/fphy.2023.1211166

Plasma-assisted CO_2 and N_2 conversion to plant nutrient

Pankaj Attri[1,2,3]*, Takamasa Okumura[3], Nozomi Takeuchi[4], Kunihiro Kamataki[3], Kazunori Koga[3,5] and Masaharu Shiratani[1,3,6,7]

[1]Center of Plasma Nano-interface Engineering, Kyushu University, Fukuoka, Japan, [2]Graduate School of Information Science and Electrical Engineering, Kyushu University, Fukuoka, Japan, [3]Faculty of Information Science and Electrical Engineering, Kyushu University, Fukuoka, Japan, [4]Department of Electrical and Electronic Engineering, Tokyo Institute of Technology, Tokyo, Japan, [5]Center for Novel Science Initiatives, National Institute of Natural Science, Tokyo, Japan, [6]Quantum and Photonics Technology Research Center, Kyushu University, Fukuoka, Japan, [7]Institute for Advanced Study, Kyushu University, Fukuoka, Japan

Colossal research on CO_2 and N_2 conversion using non-thermal plasma (NTP) technology has been ongoing since many years. The primary focus is on CO and NH_3 production through CO_2 and N_2 conversion, respectively, with high conversion efficiency and low energy consumption with or without catalysts. Although in the present study, we propose that the NTP can assist in converting CO_2 and N_2 to plant nutrients in the form of plasma-treated/activated water. We used a homemade streamer plasma device and produced plasma-activated water (PAW) using CO_2 and N_2 feed gas, CO_2-activated water (CAW) and N_2-activated water (NAW). Later, we used CAW and NAW to treat the radish seeds and evaluate the germination rate, germination percentage, and seeding growth. To understand the chemical changes in PAW after the NTP treatment, we performed a chemical analysis to detect NO_2^-, NO_3^-, NH_4^+, and H_2O_2 along with the PAW pH and temperature shift. Additionally, to understand the other species produced in the gas phase, we simulated chemical reactions using COMSOL Multiphysics® software. Our results show that NO_x and NH_x species are less produced in CAW than in NAW, but CO_2-generated PAW offers a significantly more substantial effect on enhancing the germination rate and seeding growth than NAW. Therefore, we suggested that CO and H_2O_2 formed during CAW production trigger early germination and growth enhancement. Furthermore, the total plasma reactor energy consumption, NO_3^- and NH_4^+ selective production percentage, and N_2 conversion percentage were calculated. To our best knowledge, this is the first study that uses plasma-assisted CO_2 conversion as a nutrient for plant growth.

KEYWORDS

atmospheric pressure plasma, carbon dioxide/ nitrogen conversion, plasma agriculture, simulation, plasma-activated/treated water

Introduction

Human actions such as deforestation and using fossil fuels contribute to climate change and global warming. Nitrogen is considered an essential component for supporting plant growth. The chlorophyll molecule, which gives plants the green color and powers photosynthesis, contains nitrogen. Chlorosis, or the overall yellowing of the plant, is a sign of low nitrogen levels. The catalytic function of nitrogen affects other minerals. Nitrogen fertilizers replenish the nutrients that crops lose from the soil. Crop yields and agricultural output would suffer significantly without fertilizers. Nitrogen fertilizer industries emit considerable amounts of CO_2 and other greenhouse gases. The large-scale NH_3 production still relies on the Haber–Bosch (H–B) process, which consumes 3%–5% of the world's natural gas production [1]. Around 1% of the world's greenhouse gas emission comes from NH_3 production [2].

Plasma can activate and convert atmospherically abundant N_2 into $NO_3^-$and NH_4^+, a key component of fertilizer and a necessity for agriculture. N_2 fixation is a crucial process [3, 4]. There are generally two types of resultant products from N_2 fixation by NTP, namely, NH_3 and NO_x [5–7]. Plasma-assisted NH_3 formation requires H_2 as a feedstock and usually results in a low NH_3 yield. Meanwhile, the NO_x generation route has an advantage as it directly uses air as a feeding gas to produce NO_x.

The ability of plasma technology to work at room temperature and atmospheric pressure [8–10] gives an advantage over other technology for CO_2 conversion. This technique is simple and advantageous compared to thermal procedures since reaction rates are higher and a steady state is obtained more quickly [11, 12]. There are various types of NTP technologies for CO_2 conversion such as dielectric barrier discharge (DBD) [13–15], micro-wave discharge (MWD) [16, 17], and gliding arc discharge (GAD) [18, 19].

In recent years, plasma agriculture technology has gained much attention for enhancing agricultural productivity and reducing resource loss [20–22]. Direct plasma treatment of seeds is a technique for strengthening germination and plant growth [23–26]or using plasma-activated water (PAW) for irrigation [27–34]. It has been demonstrated that PAW helps seed germination, seedling growth, and plant health [35, 36]. Direct plasma treatment and PAW treatment reduce a wide range of microorganisms, including *Leuconostoc mesenteroides*, *Saccharomyces cerevisiae*, *Escherichia coli*, and *Hafnia alvei* [37–39], drug-resistant strains of *P. aeruginosa*, *S. aureus*, and *Escherichia Coli* [40], and model yeast *Candida glabrata* [41]. Moreover, PAW treatment can upregulate the plant defense hormones like jasmonic acid and salicylic acid [42].

Sivachandiran and Khacef generated the PAW using a double-DBD reactor with synthetic air as feed gas to investigate the seed germination and plant growth in tomato, radish, and sweet pepper plants. They observed a significant impact of PAW on seed germination and plant growth [34]. Naumova et al. produced PAW using underwater electric front-type discharge with graphite rods as electrodes submerged into the solution. They reported a 50% increase in germination and root growth [33]. Lamichhane et al. developed PAW using a plasma jet with N_2 feed gas. They observed a higher germination rate and stem length in corn seeds [32]. Proto et al. used PAW produced from DBD in air. They observed a higher germination rate and plant growth for soybeans seeds [31]. Sajib et al. studied the effect of PAW produced from disk-type Cu power electrodes with an O_2 bubble. They noted a 10%–15% increase in germination for black gram seeds [30].

Lindsay et al. produced PAW by coaxial glow discharge with air as the feed gas. They irrigated marigold, tomato, and carrot branches and observed a mass increase 1.7–2.2 times that of control [29]. Zhang et al. reported a rise in lentil germination and stem growth. They used PAW produced by plasma jet with He as feed gas [28]. Terebun et al. produced PAW by using a single-phase gliding arc reactor with air feed gas. They found a beneficial effect on carrot seed germination [27]. Guragain et al. showed that PAW-treated soybean seeds had higher germination rates and increased shoot lengths and seedling lengths compared to standard water irrigation [36]. In another study, the same authors showed increased germination for radish, fenugreek, and pea seeds treated with PAW produced from a gliding arc discharge (GAD) reactor generated in the air under atmospheric pressure [43]. Zhou et al. made PAW using a plasma jet with N_2, He, air, and O_2 as feed gas to study mung bean seeds' germination and seedling growth. They observed that O_2 and air PAW-treated mung bean seeds had a higher germination index compared to N_2- and He-generated PAW-treated seeds [44]. These studies suggested that PAW can improve plant growth, mainly when air is used as feeding gas.

Limited studies were reported where multiple feed gases were used to produce and test PAW on seeds. To our best knowledge, the treatment of plant seeds using CO_2 feed gas plasma-produced PAW has not been studied yet. Therefore, in the present study, we used CO_2 and N_2 feed gas plasma to create PAW and tested them on the brown radish seeds. We evaluated the germination rate, percentage, and seedling growth. Additionally, we focused on the plasma chemistry generated by CO_2 and N_2 plasma to understand the mechanism behind the enhanced germination and seedling growth.

Materials and methods

Preparation of CO_2-generated PAW and N_2-generated PAW

We have built a homemade streamer discharge plasma reactor, as shown in Figure 1. The distance between the needle tip and the water surface was set at 3 mm. We applied a continuous sinusoidal voltage of 6.9 and 11 kVp-p with a frequency of 24 kHz to the SUS needle electrode fixed at the outlet of the gas tube on 5 mL of water to produce CO_2-activated water (CAW) and N_2-activated water (NAW). We grounded the water through a glass layer that worked as an insulating material, preventing any arc transition. We supplied CO_2 and N_2 with a purity of 99.99% to the reactor through a gas tube with a diameter of 4.35 mm at a flow rate of 0.5 L/min. The total power of the plasma reactor was measured using a Watt monitor (TAP-TST8N), Sanwa Supply Inc., Okayama, Japan. The power was 10 and 13 W for CAW and NAW production, respectively [45, 46].

Seed treatment and germination

We bought radish (*Raphanus sativus* L.) seeds from Nakahara Seed Co., Japan, 2018, and stored them at 4 °C. We used control and plasma-treated radish seeds (8 replicates × 30 seeds × 2 times = 480 seeds) for the experiments. The 30 seeds were placed in a 90 cm Petri dish lined with Whatman filter paper. 6 mL of DI water (Control), CAW, and NAW were added to each Petri dish, as shown in Figure 1. The Petri dishes with seeds were kept in a dark incubator for 24 h at 25 °C temperature. The number of germinated seeds was counted eight times (6, 10, 12, 14, 16, 18, 20, and 24 h) after imbibition. Afterward, the morphometric analysis of sprouts was performed for all conditions.

10.3389/fphy.2023.1211166

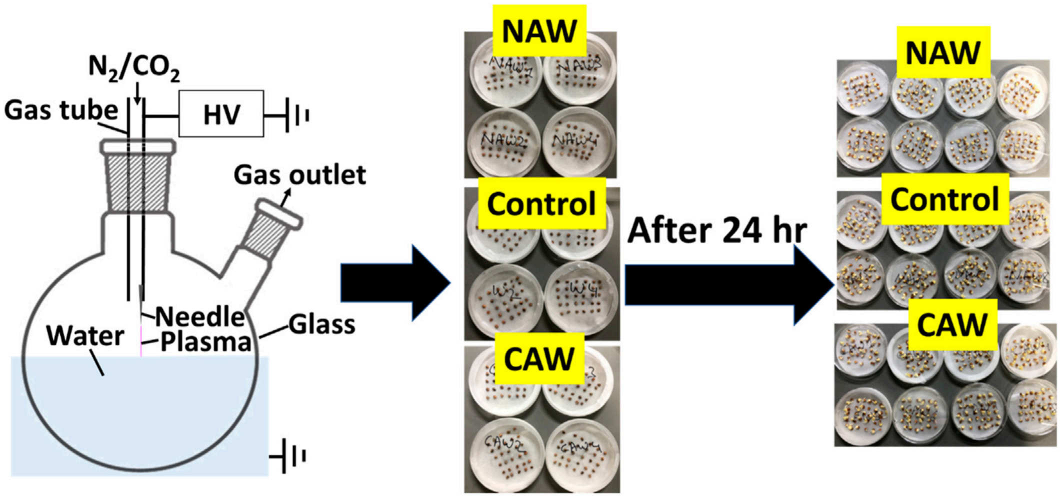

FIGURE 1
Schematic depiction of the study.

Chemical analysis, pH change, reactor temperature, and energy consumption in CAW and NAW production

We used the NO_2/NO_3 assay kit from Dojindo Laboratories, Japan, to analyze the concentration of NO_2^- and NO_3^- in PAW. The concentration of NH_4^+ in PAW was analyzed from the ammonia assay kit-modified Berthelot from Abcam company. H_2O_2 was measured using a Pack Test analysis kit, model WAK-H_2O_2, from KYORITSU CHEMICAL-CHECK Lab., Corp., Japan. PAW pH was measured using a HORIBA LAQUA F-72 Benchtop pH/ORP/Ion/Temperature Meter. We used AS One Thermography TIM-03 (accuracy of ± 2° C), which measures temperature using infrared radiation, to measure the change in water temperature after plasma irradiation. The total plasma reactor energy consumption (PREC), PREC for NO_3^- fixation, PREC for NH_4^+ fixation, percentage of NH_4^+ selectivity, percentage of NO_3^- selectivity, and percentage of total N_2 conversion [47] are as shown in Eqs (1–8).

The total PREC for total N fixation (NO_3^- + NH_4^+) is

$$EC\left(\frac{\mathrm{MJ}}{\mathrm{mol}}\right) = \frac{Power}{Moles\ [NO_3^- + NH_4^+]\, per\ second\ [mol.s^{-1}]} \times \frac{1}{10^6\ \left[\frac{J}{MJ}\right]}, \tag{1}$$

$$PREC\, of\ only\ Nitrogen\ flow\left(\frac{\mathrm{MJ}}{\mathrm{mol}}\right) = \frac{Power}{Moles\ [c(NO_3^- + NH_4^+) for\ N_2\ flow - c(NO_3^- + NH_4^+) for\ CO_2\ flow]\, per\ second\ [mol.s^{-1}]} \times \frac{1}{10^6\ \left[\frac{J}{MJ}\right]}. \tag{2}$$

The PREC for NO_3^- fixation of only nitrogen flow is

$$EC\left(\frac{\mathrm{MJ}}{\mathrm{mol}}\right) = \frac{Power}{Moles\ [c(NO_3^-) for\ N_2\ flow - c(NO_3^-) for\ CO_2\ flow]\, per\ second\ [mol.s^{-1}]} \times \frac{1}{10^6\ \left[\frac{J}{MJ}\right]}. \tag{3}$$

The PREC for NH_4^+ fixation of only nitrogen flow is

$$EC\left(\frac{\mathrm{MJ}}{\mathrm{mol}}\right) = \frac{Power}{Moles\ [c(NH_4^+) for\ N_2\ flow - c(NH_4^+) for\ CO_2\ flow]\, per\ second\ [mol.s^{-1}]} \times \frac{1}{10^6\ \left[\frac{J}{MJ}\right]}. \tag{4}$$

The percentage of NH_4^+ selectivity for only nitrogen flow is

$$\%\ of\ NH_4^+\ \text{selectivity} = \frac{c(NH_4^+)}{c(NH_4^+ + NO_3^-)} \times 100\,\%. \tag{5}$$

The percentage of NO_3^- selectivity for only nitrogen flow is

$$\%\ of\ NH_4^+\ \text{selectivity} = \frac{c(NO_3^-)}{c(NH_4^+ + NO_3^-)} \times 100\,\%. \tag{6}$$

The percentage of total N_2 conversion is

$$\%\, of\ total\ N_2\ conversion = \frac{c(NH_4^+ + NO_3^-) mol/L}{5\, min} \times Solution\ volume\ (L) \times 24.5 \frac{L}{mol} \times \frac{1}{0.5\ L/min} \times 100\,\%. \tag{7}$$

The percentage of total N_2 conversion for only nitrogen flow is

$$\%\, of\ total\ N_2\ conversion = \frac{c[(c(NO_3^-) for\ N_2\ flow - c(NO_3^-) for\ CO_2\ flow) mol/L]}{5\, min} \times Solution\ volume\ (L) \times 24.5 \frac{L}{mol} \times \frac{1}{0.5\ L/min} \times 100\,\%. \tag{8}$$

Zero-spatial dimension simulation using COMSOL Multiphysics® software

In this study, the COMSOL Multiphysics® Chemical Reaction Engineering Module, version 5.6, was used. The Model Wizard was

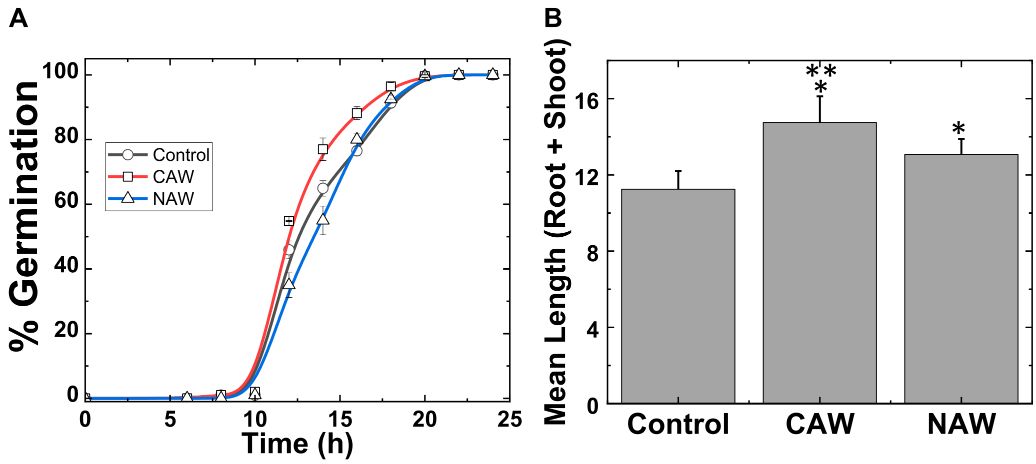

FIGURE 2
(A) Rate of germination of radish sprouts after DI water, CAW, and NAW treatment and **(B)** mean length (root + shoot) changed after CAW and NAW treatment. Results are presented as means ± SEM.*Significantly different from the control group (p < 0.05). **CAW group significantly differs from the NAW group (p < 0.05).

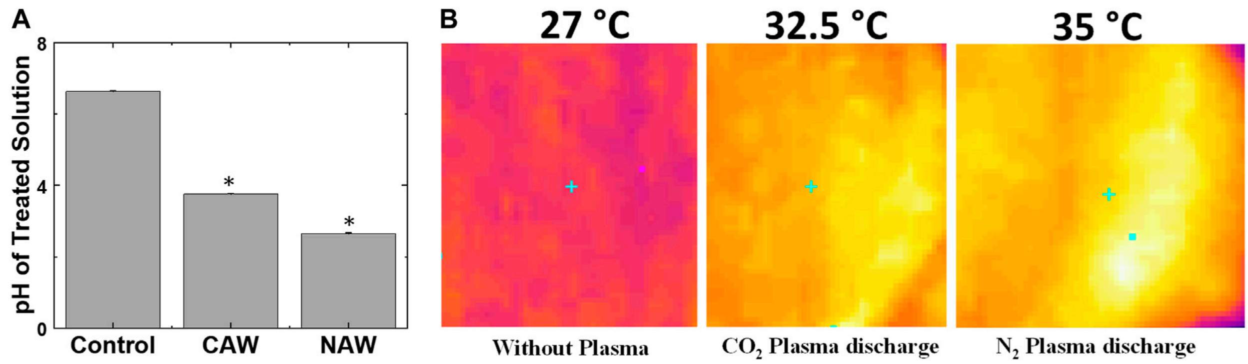

FIGURE 3
(A) Change in pH of the solution after CO_2 and N_2 feed gas plasmas and **(B)** change in water temperature before and after CO_2 and N_2 plasmas. *Significantly different from the control group (p < 0.05).

TABLE 1 Germination rate of radish sprouts in the presence of CAW and NAW treatment.

Incubation time (h)	% germination in control	% germination in CAW-treated seeds	% germination in NAW-treated seeds
0	0	0	0
12	46	55	35
14	65	77	55
16	77	88	80
18	91	96	92
20	100	100	100

chosen with a time-dependent analysis and zero spatial dimension (0D). The simulation was calculated based on input parameters entered under Global Definition, as explained in the following section. For the 0D model, we calculated the mean electron temperature of 1.22 eV for CO_2 plasma using the LXCat program with the BOLSIG+ and Phelps databases [48–50]. We used an electron number density of $10^{16}\ m^{-3}$ and a gas temperature of 600 K as the input in the model. Spyrou et al. reported the temperature distribution of nitrogen-neutral molecules in a secondary streamer discharge [51]. They observed that the

TABLE 2 Mean total length of radish sprouts in the presence of CAW and NAW treatment.

Treatment condition	Mean total length of radish sprouts
Control	11 ± 0.9 cm
CAW	15 ± 1.0 cm
NAW	13 ± 0.8 cm

neutral gas temperature reached 800 K near the point electrode at a distance of 0.5 mm. As the distance from the electrode increased, the temperature decreased and remained constant at around 450 K [51]. Additionally, Komuro et al. performed a 2D simulation of atmospheric pressure streamer discharge at 600 K gas temperature in humid air [52]. In the simulation, we assumed a gas temperature of 600 K and an electron density of 10^{16} m^{-3}.

Additionally, we included 0.2 fractions of H_2O and 0.8 fractions of N_2 in the CO_2 plasma simulation. In the N_2 plasma simulation, we kept the water value fraction the same as in CO_2 plasma and did not add any CO_2 fraction. As shown in Figure 1, the discharge was performed on water, which resulted in water vaporization, so we included water in the simulation. The presence of N_2 is included because our reactor is open from one end (see Figure 1), so air interferes with the CO_2 flow (0.5 L/min). Therefore, we added our assumption parts of H_2O and N_2 in the simulation. We ran the chemical reaction for the residence time of 300 s. The rate constants were compiled from the literature described in Supplementary Table S1 (Supplementary Material).

Result and discussion

Germination rate and seedling growth in the presence of DI water, CAW, and NAW

The radish seeds were harvested in 2018 and stored at room temperature (4 °C). We standardized the optimal plasma treatment time for 5 min to prepare the CAW and NAW in the present study. The optimal use of time was found through a different experiment. Figure 2A and Table 1 show that control seeds (DI water), CAW-treated seeds, and NAW-treated seeds showed maximal germination of 100% after 24 h. However, 50% of seeds germinated in control after 13 h, for NAW, after 13.5 h, and for CAW, after 12 h of imbibition. Table 1 shows rapid germination in CAW-treated seeds. 50% of seeds germinated with NAW treatment showed lower germination compared to the control, although both NAW and control showed 100% germination after 20 h (Figure 2A). While higher germination was observed for CAW up to 18 h, later, 100% germination showed for all treatment conditions. The results indicate that the PAW affects germination kinetics, depending on the feed gas. This suggests that the concentration of ROS (reactive oxygen species) and RNS (reactive nitrogen species) plays a significant factor in 50% of seeds early germinated in CAW and delayed in NAW.

Figure 2B and Table 2 show the change in the mean total length of sprouts (root + shoot) before and after plasma treatment for all treatment conditions. The average length of sprouts for the control seeds was 11 ± 0.9 cm, whereas after the CAW treatment, it was 15 ± 1.0 cm, and after NAW treatment, it was 13 ± 0.8 cm (Figure 2B). The average length of sprouts after CAW and NAW treatment was significantly higher than in the control (Figure 2B). For CAW- and NAW-treated seeds, the length of sprouts increased by 26% and 15% compared to the control ($p < 0.05$), respectively (Figure 2B). Additionally, the length of sprouts treated with CAW was 13% higher than that of NAW-treated sprouts ($p < 0.05$). We performed physical and chemical analyses of the PAW to understand this behavior of CAW.

Change in the pH and temperature of the reactor and chemical analysis in PAW

Figure 3A shows the change in pH for CAW and NAW compared to the control. The control DI water has a pH of 6.6, but after the plasma treatment for 5 min using the CO_2 feed gas, the pH decreases to 3.8, while the pH for nitrogen feed gas plasma-treated water reduces to 2.6. Zhang et al. investigated the germination rate of radish seeds soaked in electrolyzed oxidizing (EO) water with different pH values (2.5, 3.5, 4.5, 5.5, and 6.5). They observed that seeds soaked at pH 6.5 showed a slightly higher germination rate compared to those soaked at other pH values [53]. This suggests that the difference in pH between CAW and NAW does not account for the faster germination of CAW-treated seeds. Guragain et al. mentioned that the plasma treatment for 20 min lowered the pH of deionized water from 6.40 to 4.26. However, treating radish and pea seeds with PAW (pH 4.26) increased their germination to 100% and 79%, compared to 93% and 64% for seeds treated with deionized water (pH 6.40), respectively [43]. Later, we measured the plasma-treated water temperature changes, as seen in Figure 3B. There was a 5 °C increase in the water temperature for CO_2 feed gas plasma. In contrast, an 8 °C increase in water temperature was obtained after N_2 feed gas plasma.

Furthermore, to understand the reason behind the decrease in pH, we measured the concentration of NO_2^-, NO_3^-, and NH_4^+ in water after treatment with CO_2 and N_2 feed gas plasma. The NO_2^- concentration was 0.12 ± 0.09 μM for the CO_2-treated solution, but we could not detect any NO_2^- concentration in the N_2-treated water (Figure 4A). We also observed the change in NO_3^- concentration in water after CO_2 and N_2 plasma treatment (Figure 4B). The NO_3^- concentration was 13 ± 0.1 μM in CAW and 216 ± 5.0 μM in NAW. As expected, we detected more NO_3^- in N_2 plasma than in CO_2 plasma. The presence of NO_3^- in CO_2 plasma was due to the interference of air as one end of the reactor is open. We also measured the concentration of NH_4^+ produced in the water after plasma treatment with both CO_2 and N_2 feed gases.

Figure 4C shows that NH_4^+ concentration in CAW was 10.9 ± 4.3 μM, whereas the concentration of NH_4^+ in NAW was 61.47 ± 1.4 μM. Our reactor could generate both NO_3^- and NH_4^+ without H_2 feed gas. To calculate the concentration of NO_3^- and NH_4^+ explicitly produced by the N_2 flow, we subtracted the NO_3^- and NH_4^+ concentrations of CAW from those of NAW to avoid the role of excess atmospheric N_2 gas in the reactor. After subtraction, we obtained 202.6 and 50.5 μM concentrations for NO_3^- and NH_4^+, respectively, for only N_2 flow plasma. We also detected H_2O_2 concentrations of 714.3 ± 8.6 and 321.4 ± 2.7 μM in CAW and NAW, respectively (Figure 4D). This indicates that CAW had approximately twice as much H_2O_2 as NAW.

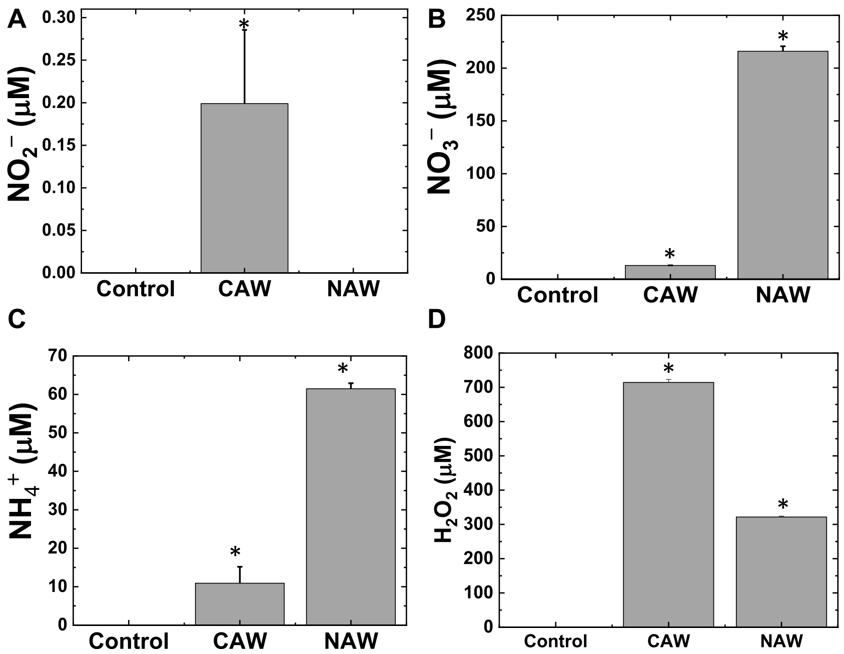

FIGURE 4
Production of reactive species in water after CO_2 and N_2 feed gas plasmas. **(A)** NO_2^-, **(B)** NO_3^-, **(C)** NH_4^+, and **(D)** H_2O_2. *Significantly different from the control group (p < 0.05).

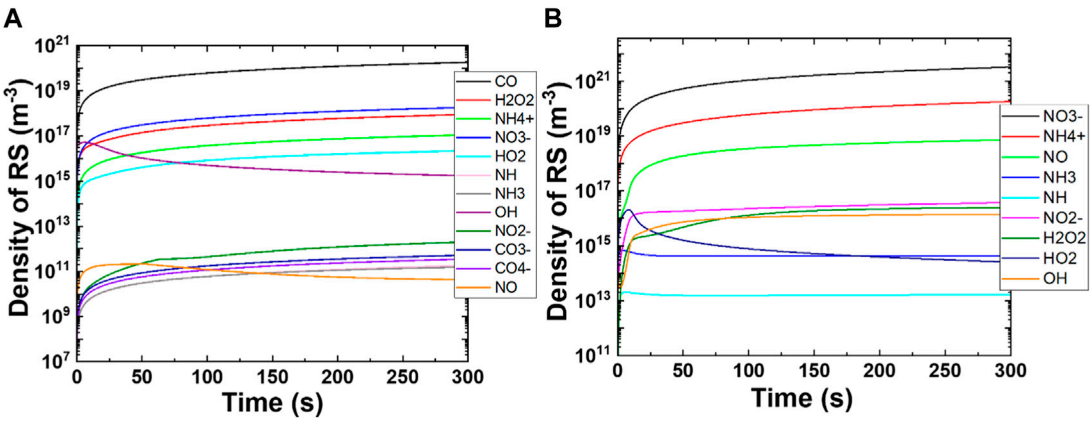

FIGURE 5
Change in the production of reactive species densities as the function of time. **(A)** CO_2 feed gas plasma and **(B)** N_2 feed gas plasma.

To closely understand the difference in the production of NO_2^-, NO_3^-, NH_4^+, and H_2O_2, we performed the simulation as follows.

Change in the density of reactive species with CO_2 and N_2 feed gas plasma

To understand the changes in reactive species production as a function of time, we performed 0D simulation using COMSOL Multiphysics® simulation software, with 376 reactions and 81 species (neutral and ions). Many short- and long-lived ROS and RNS species are generated during the 300 s simulation; the time-dependent changes in the radical densities of reactive species are shown in Figure 5. We have not included species with densities less than 10^6 m^{-3} in Figure 5.

Figure 5A shows the changes in the density of reactive species as a function of time in CO_2 plasma. We focused on the reactive species in Figure 5A that had densities higher than 10^6 m^{-3} like CO, CO_3^-, CO_4^-, H_2O_2, HO_2, OH, NH, NH_3, NH_4^+, NO, NO_2^-, and NO_3^-. As we expected, the density of CO was the highest among all the reactive species of 10^{20} m^{-3}, followed by NO_3^-, NH_4^+ (10^{18} m^{-3} each), and H_2O_2 (10^{17} m^{-3}). The CO density increases as the simulation time increases and becomes almost constant after the 250 s simulation. The densities of CO, CO_3^-, CO_4^-, H_2O_2, HO_2, NH, NH_3, NH_4^+, NO_2^-, and NO_3^- species increase as the simulation time increases, whereas the densities of OH and NO first increase and later decrease. The decrease in OH density after 10 s simulation was sharp, while the decrease in NO density was smoother. This shows that short-lived species like OH and NO were generated in early simulation and later converted to long-lived species like H_2O_2, HO_2, NO_2^-, and NO_3^-. The simulation results revealed that CO_2 plasma could effectively produce CO, OH, H_2O_2, HO_2, NH_4^+, NO, NO_2^-, and NO_3^- with medium to high densities that were helpful in plant growth.

Figure 5B shows the time depended on changes in the density of reactive species with N_2 plasma in the presence of water. N_2 plasma generated both ROS and RNS with medium (>10^6 m^{-3}) to high (>10^{21} m^{-3}) densities. The simulation results showed the highest increase in densities of NH_4^+ and NO_3^- to 10^{20} and 10^{21} m^{-3}, respectively, after 300 s simulation. The highest density was obtained for NO_3^-, and the density was increased as the simulation time increased. Similar behavior was observed for NH_4^+, H_2O_2, OH, NH_4^+, NO, and NO_2^-. The densities of HO_2, NH, and NH_3 increased first for 10 s simulation and later decreased. The decrease in NH and NH_3 densities contributed to the production of NH_4^+, while a decrease in HO_2 density contributed to the formation of H_2O and OH (see Supplementary Table S1).

These simulation results reveal that CO_2 feed gas plasma produces not only CO with a high density but also ROS and RNS parallelly. Interestingly, the densities of RNS species like NH_4^+ and NO_3^- are very similar, which correlate well with our experimental results. In the wet experiments (the previous section), we obtained almost similar concentrations of NH_4^+ and NO_3^- in CAW. Hence, our experimental results were consistent with the simulation results. Moreover, N_2 plasma had higher NOx and NHx species concentrations compared to ROS. We assume that the concentration of ROS and RNS produced in the gas phase dissolved in water at a similar ratio (depending on Henry's constant). Therefore, the concentrations of species in water are close approximations of those in the gas phase.

Later we calculated the total PREC, NH_4^+ and NO_3^- selective production, and N_2 conversion for N_2 feed gas plasma.

Total plasma reactor energy consumption, percentage of NH_4^+ and NO_3^- selective production, and N_2 conversion percentage

The total PREC for N_2 conversion to NO_3^- and NH_4^+ using Eq (1) with N_2 feed gas was 2837 MJ/mol, while the PREC for CO_2 feed gas for N_2 conversion was 30620 MJ/mol. As discussed above, the presence of N_2 in the reactor or dissolved N_2 in the water caused the production of NH_4^+, NO_2^-, and NO_3^- in the CO_2 feed gas plasma. We used Eq 2 to evaluate the total PREC of only N_2 flow and obtained a PREC value of 3127 MJ/mol. We also assessed the PREC for NO_3^- and NH_4^+ conversion for only N_2 flow as 3908 and 15663 MJ/mol, respectively. Later, we calculated the percentage of selective production of NH_4^+ and NO_3^- from Eqs 3, 4, which was 20% and 80%, respectively. Furthermore, we calculated the total N_2 conversion using Eqs 7, 8 as 0.0013% and 0.0012%, respectively, for N_2 feed gas plasma. In an earlier study, N_2 plasma jet containing 5–10% H_2O vapor discharged on 5 mL water resulted in 95% NH_3 production with 0.0008% N_2 conversion without a catalyst [47]. In the reported work, the feed gas with H_2O vapor (5–10%) was introduced in the plasma jet, while we did not introduce water vapor with the feed gas in the present study.

The results show that the difference in the concentration of RNS and ROS between CO_2 and N_2 feed gas plasma can cause a difference in germination and seedling growth, as shown in the previous section. Our germination results correlate well with a prior report by Zhou et al., where they provided evidence that O_2 and air PAW are more efficient in enhancing the germination of mung bean than N_2-produced PAW [44]. They explained that the high density of ROS generated in air and O_2 plasma was responsible for the enhanced germination in mung beans [44].

The high concentration of RNS in N_2 plasma was apparently due to the substantial presence of N_2. Meanwhile, ROS production was higher in CO_2 plasma because the production of O by dissociation from CO_2 could react with water vapor to produce H_2O_2. The high concentration of H_2O_2 production in CAW compared to NAW also contributed to the early germination and seedling growth. Wojtyla et al. reported that H_2O_2 was required for numerous signaling activities throughout the plant life cycle [54]. They also stated that applying H_2O_2 externally could increase seed germination [55, 56].

In recent years, CO has been demonstrated to belong to the most critical cellular elements influencing a broad range of biological processes across plants and animals [57]. CO acts as a compound that affects seed germination [58], inducing stomatal closure [59] and root development [60]. In addition, Wang and Liao mentioned that signaling molecules like NO, phytohormones (IAA, ABA, and GA), H_2O_2, and other gas signaling molecules exhibit cross-talk with CO [61]. As shown above, the pH of CAW is 3.8. It is highly possible that the dissolved CO can convert to a stable acid solution such as formic acid and carbonic acid in a CAW solution. Fan et al. demonstrated the electrochemical CO_2 reduction to formic acid solutions [62]. As previously reported, the combination of NH_4^+ and NO_3^- is better for plant growth than NH_4^+ or NO_3^- alone [63]. Hence, CO with H_2O_2, NO_3^-, and NH_4^+ added the secret ingredient to the cocktail of reactive species in CAW, resulting in enhanced germination and seeding growth compared to NAW and control. Although the total PREC for N_2 conversion is high in our reactor, in our future study, we will focus on decreasing the PREC of the reactor to make it more feasible for commercialization. Douat et al. showed for the first time the medical application of CO generated by a He plasma jet with a 1% CO_2 admixture [64], and our study showed the role of plasma-generated CO in agriculture for the first time.

Conclusion

In this investigation, we have shown that CO_2 and N_2 can be converted to plant nutrients in the form of H_2O_2, NO_3^-, NH_4^+, and CO, which helps germinate and grow radish sprouts. We found that adding CO in CAW enhanced early germination and seedling growth. NAW has a high concentration of RNS even though NAW-treated seeds showed a lower germination rate. By contrast, the CAW solution has less RNS but more ROS, especially H_2O_2 and CO, resulting in early germination and seedling growth of radish sprouts. We conclude that RNS is vital for plant growth, but ROS and CO can accelerate plant growth. Finally, we suggest that plasma-assisted CO_2 and N_2 conversion to plant nutrients is a valuable alternative that can increase agricultural products and reduce carbon emission.

Data availability statement

The original contributions presented in the study are included in the article/Supplementary Material; further inquiries can be directed to the corresponding author.

Author contributions

Conceptualization and writing—original draft preparation: PA; simulations: PA and NT; plasma reactor design and analysis: TO; and review and editing: KKa, KKo, and MS. All authors contributed to the article and approved the submitted version.

Funding

This work was supported by the JSPS-KAKENHI, grant number 22H01212. Additionally, it was partly funded by the JSPS-KAKENHI (grant numbers JP16H03895, JP19H05462, JP19K14700, JP20H01893, and JP20K14454) and JSPS Core-to-Core Program "Data Driven Plasma Science," (grant number JPJSCCA2019002), Plasma Bio Consortium, and Center for Low-temperature Plasma Sciences (cLPS), Nagoya University.

Conflict of interest

The authors declare that the research was conducted in the absence of any commercial or financial relationships that could be construed as a potential conflict of interest.

Publisher's note

Supplementary material

The Supplementary Material for this article can be found online at: https://www.frontiersin.org/articles/10.3389/fphy.2023.1211166/full#supplementary-material

References

1. Wang L, Xia M, Wang H, Huang K, Qian C, Maravelias CT, et al. Greening ammonia toward the solar ammonia refinery. *Joule* (2018) 2:1055–74. doi:10.1016/J.JOULE.2018.04.017

2. MacFarlane DR, Cherepanov PV, Choi J, Suryanto BHR, Hodgetts RY, Bakker JM, et al. A roadmap to the ammonia economy. *Joule* (2020) 4:1186–205. doi:10.1016/J.JOULE.2020.04.004

3. Islam MA, Adjesiwor AT, Islam MA, Adjesiwor AT. Nitrogen fixation and transfer in agricultural production systems. In: *Nitrogen in agriculture - updates* (2017). doi:10.5772/INTECHOPEN.71766

4. Vance CP, Graham PH. Nitrogen fixation in agriculture: Application and perspectives. In: *Nitrogen fixation: Fundamentals and applications* (1995). p. 77–86. doi:10.1007/978-94-011-0379-4_10

5. Vervloessem E, Gorbanev Y, Nikiforov A, De Geyter N, Bogaerts A. Sustainable NOx production from air in pulsed plasma: Elucidating the chemistry behind the low energy consumption. *Green Chem* (2022) 24:916–29. doi:10.1039/D1GC02762J

6. Kumari S, Pishgar S, Schwarting ME, Paxton WF, Spurgeon JM. Synergistic plasma-assisted electrochemical reduction of nitrogen to ammonia. *Chem Commun* (2018) 54:13347–50. doi:10.1039/C8CC07869F

7. Wu A, Yang J, Xu B, Wu XY, Wang Y, Lv X, et al. Direct ammonia synthesis from the air via gliding arc plasma integrated with single atom electrocatalysis. *Appl Catal B* (2021) 299:120667. doi:10.1016/J.APCATB.2021.120667

8. Chen H, Mu Y, Hardacre C, Fan X. Integration of membrane separation with nonthermal plasma catalysis: A proof-of-concept for CO2 capture and utilization. *Ind Eng Chem Res* (2020) 59:8202–11. doi:10.1021/acs.iecr.0c01067

9. George A, Shen B, Craven M, Wang Y, Kang D, Wu C, et al. A review of non-thermal plasma technology: A novel solution for CO2 conversion and utilization. *Renew Sustain Energ Rev* (2021) 135:109702. doi:10.1016/J.RSER.2020.109702

10. Bogaerts A, Centi G. Plasma technology for CO2 conversion: A personal perspective on prospects and gaps. *Front Energ Res* (2020) 8:111. doi:10.3389/fenrg.2020.00111

11. Ashford B, Tu X. Non-thermal plasma technology for the conversion of CO2. *Curr Opin Green Sustain Chem* (2017) 3:45–9. doi:10.1016/J.COGSC.2016.12.001

12. Marcantonio V, De Falco M, , Bocci E. 2022 Non-thermal plasma technology for CO2 conversion—an overview of the most relevant experimental results and kinetic models. *Energies* 15, 7790. doi:10.3390/EN15207790

13. Wang XC, Bai JX, Zhang TH, Sun Y, Zhang YT. Comprehensive study on discharge characteristics in pulsed dielectric barrier discharges with atmospheric He and CO2. *Phys Plasmas* (2022) 29:083503. doi:10.1063/5.0096172

14. Duan X, Li Y, Ge W, Wang B. Degradation of CO2 through dielectric barrier discharge microplasma. *Greenhouse Gases: Sci Technol* (2015) 5:131–40. doi:10.1002/GHG.1425

15. Paulussen S, Verheyde B, Tu X, De Bie C, Martens T, Petrovic D, et al. Conversion of carbon dioxide to value-added chemicals in atmospheric pressure dielectric barrier discharges. *Plasma Sourc Sci Technol* (2010) 19:034015. doi:10.1088/0963-0252/19/3/034015

16. Chun SM, Shin DH, Ma SH, Yang GW, Hong YC. CO2 microwave plasma—catalytic reactor for efficient reforming of methane to syngas. *Catalysts* (2019) 9:292. doi:10.3390/CATAL9030292

17. Britun N, Silva T, Chen G, Godfroid T, Van Der Mullen J, Snyders R. Plasma-assisted CO2 conversion: Optimizing performance via microwave power modulation. *J Phys D Appl Phys* (2018) 51:144002. doi:10.1088/1361-6463/AAB1AD

18. Slaets J, Aghaei M, Ceulemans S, Van Alphen S, Bogaerts A. CO2 and CH4 conversion in "real" gas mixtures in a gliding arc plastron: How do N2 and O2 affect the performance? *Green Chem* (2020) 22:1366–77. doi:10.1039/C9GC03743H

19. Trenchev G, Kolev S, Wang W, Ramakers M, Bogaerts A. CO2 conversion in a gliding Arc plastron: Multidimensional modeling for improved efficiency. *J Phys Chem C* (2017) 121. doi:10.1021/acs.jpcc.7b08511

20. Attri P, Ishikawa K, Okumura T, Koga K, Shiratani M. Plasma agriculture from laboratory to farm: A review. *Processes* (2020) 8:1002. doi:10.3390/pr8081002

21. Koga K, Attri P, Kamataki K, Itagaki N, Shiratani M, Mildaziene V. Impact of radish sprouts seeds coat color on the electron paramagnetic resonance signals after plasma treatment. *Jpn J Appl Phys* (2020) 59:SHHF01. doi:10.35848/1347-4065/ab7698

22. Attri P, Okumura T, Koga K, Shiratani M, Wang D, Takahashi K, et al. Outcomes of pulsed electric fields and nonthermal plasma treatments on seed germination and protein functions. *Agronomy* (2022) 12:482. doi:10.3390/agronomy12020482

23. Sarinont T, Amano T, Attri P, Koga K, Hayashi N, Shiratani M. Effects of plasma irradiation using various feeding gases on growth of Raphanus sativus L. *Arch Biochem Biophys* (2016) 605:129–40. doi:10.1016/j.abb.2016.03.024

24. Attri P, Ishikawa K, Okumura T, Koga K, Shiratani M, Mildaziene V. Impact of seed color and storage time on the radish seed germination and sprout growth in plasma agriculture. *Sci Rep* (2021) 11:2539. doi:10.1038/s41598-021-81175-x

25. Suriyasak C, Hatanaka K, Tanaka H, Okumura T, Yamashita D, Attri P, et al. Alterations of DNA methylation caused by cold plasma treatment restore delayed germination of heat-stressed rice (oryza sativa L.) seeds *ACS Agric Sci Technol* (2021) 1: 5–10. doi:10.1021/acsagscitech.0c00070

26. Okumura T, Attri P, Kamataki K, Yamashita N, Tsukada Y, Itagaki N, et al. Detection of NO3− introduced in plasma-irradiated dry lettuce seeds using liquid chromatography-electrospray ionization quantum mass spectrometry (LC-ESI QMS). *Scientific Rep* (2022) 12:12525. doi:10.1038/s41598-022-16641-1

27. Terebun P, Kwiatkowski M, Hensel K, Kopacki M, Pawłat J. Influence of plasma activated water generated in a gliding arc discharge reactor on germination of beetroot and carrot seeds. *Appl Sci* (2021) 11:6164. doi:10.3390/APP11136164

28. Zhang S, Rousseau A, Dufour T. Promoting lentil germination and stem growth by plasma activated tap water, demineralized water and liquid fertilizer. *RSC Adv* (2017) 7: 31244–51. doi:10.1039/C7RA04663D

29. Lindsay A, Byrns B, King W, Andhvarapou A, Fields J, Knappe D, et al. Fertilization of radishes, tomatoes, and marigolds using a large-volume atmospheric glow discharge. *Plasma Chem Plasma Process* (2014) 34:1271–90. doi:10.1007/s11090-014-9573-x

30. Sajib SA, Billah M, Mahmud S, Miah M, Hossain F, Omar FB, et al. Plasma activated water: The next generation eco-friendly stimulant for enhancing plant seed germination, vigor and increased enzyme activity, a study on black gram (vigna mungo L.) *Plasma Chem Plasma Process* (2020) 40:119–43. doi:10.1007/s11090-019-10028-3

31. Lo Porto C, Ziuzina D, Los A, Boehm D, Palumbo F, Favia P, et al. Plasma activated water and airborne ultrasound treatments for enhanced germination and growth of soybean. *Innovative Food Sci Emerging Tech* (2018) 49:13–9. doi:10.1016/J.IFSET.2018.07.013

32. Lamichhane P, Veerana M, Lim JS, Mumtaz S, Shrestha B, Kaushik NK, et al. Low-temperature plasma-assisted nitrogen fixation for corn plant growth and development. *Int J Mol Sci* (2021) 22:5360 doi:10.3390/IJMS22105360

33. Naumova IK, Maksimov AI, Khlyustova AV. Stimulation of the germinability of seeds and germ growth under treatment with plasma-activated water. *Surf Eng Appl Electrochem* (2011) 47:263–5. doi:10.3103/s1068375511030136

34. Sivachandiran L, Khacef A. Enhanced seed germination and plant growth by atmospheric pressure cold air plasma: Combined effect of seed and water treatment. *RSC Adv* (2017) 7:1822–32. doi:10.1039/C6RA24762H

35. Waskow A, Howling A, Furno I. Mechanisms of plasma-seed treatments as a potential seed processing technology. *Front Phys* (2021) 9:174. doi:10.3389/fphy.2021.617345

36. Guragain RP, Baniya HB, Dhungana S, Chhetri GK, Sedhai B, Basnet N, et al. Effect of plasma treatment on the seed germination and seedling growth of radish (Raphanus sativus). *Plasma Sci Technol* (2021) 24:015502. doi:10.1088/2058-6272/AC3476

37. Kamgang-Youbi G, Herry JM, Brisset JL, Bellon-Fontaine MN, Doubla A, Naïtali M. Impact on disinfection efficiency of cell load and of planktonic/adherent/detached state: Case of Hafnia alvei inactivation by Plasma Activated Water. *Appl Microbiol Biotechnol* (2008) 81:449–57. doi:10.1007/s00253-008-1641-9

38. Kamgang-Youbi G, Herry JM, Meylheuc T, Brisset JL, Bellon-Fontaine MN, Doubla A, et al. Microbial inactivation using plasma-activated water obtained by gliding electric discharges. *Lett Appl Microbiol* (2009) 48:13–8. doi:10.1111/J.1472-765X.2008.02476.X

39. Naítali M, Kamgang-Youbi G, Herry JM, Bellon-Fontaine MN, Brisset JL. Combined effects of long-living chemical species during microbialinactivation using atmospheric plasma-treated water. *Appl Environ Microbiol* (2010) 76:7662–4. doi:10.1128/AEM.01615-10

40. Maho T, Binois R, Brulé-Morabito F, Demasure M, Douat C, Dozias S, et al. Anti-bacterial action of plasma multi-jets in the context of chronic wound healing. *Appl Sci* (2021) 11:9598. doi:10.3390/APP11209598

41. Trebulová K, Krčma F, Kozáková Z, Matoušková P. Impact of microwave plasma torch on the yeast Candida glabrata. *Appl Sci* (2020) 10:5538. doi:10.3390/APP10165538

42. Adhikari B, Adhikari M, Ghimire B, Park G, Choi EH. Cold atmospheric plasma-activated water irrigation induces defense hormone and gene expression in tomato seedlings. *Sci Rep* (2019) 9:16080. doi:10.1038/s41598-019-52646-z

43. Guragain RP, Baniya HB, Pradhan SP, Pandey BP, Subedi DP. Influence of plasma-activated water (PAW) on the germination of radish, fenugreek, and pea seeds. *AIP Adv* (2021) 11:125304. doi:10.1063/5.0070800

44. Zhou R, Li J, Zhou R, Zhang X, Yang S. Atmospheric-pressure plasma treated water for seed germination and seedling growth of mung bean and its sterilization effect on mung bean sprouts. *Innovative Food Sci Emerging Tech* (2019) 53:36–44. doi:10.1016/J.IFSET.2018.08.006

45. Attri P, Koga K, Okumura T, Takeuchi N, Shiratani M. Green route for ammonium nitrate synthesis: Fertilizer for plant growth enhancement. *RSC Adv* (2021) 11:28521–9. doi:10.1039/D1RA04441A

46. Xu M, Fukuyama Y, Nakai K, Liu Z, Sumiya Y, Okino A. Characteristics of double-layer, large-flow dielectric barrier discharge plasma source for toluene decomposition. *Plasma* (2023) 6:212–24. doi:10.3390/PLASMA6020016

47. Gorbanev Y, Vervloessem E, Nikiforov A, Bogaerts A. Nitrogen fixation with water vapor by nonequilibrium plasma: Toward sustainable ammonia production. *ACS Sustain Chem Eng* (2020) 8:2996–3004. doi:10.1021/acssuschemeng.9b07849

48. Hagelaar GJM, Pitchford LC. Solving the Boltzmann equation to obtain electron transport coefficients and rate coefficients for fluid models. *Plasma Sourc Sci Technol* (2005) 14:722–33. doi:10.1088/0963-0252/14/4/011

49. Pitchford LC, Alves LL, Bartschat K, Biagi SF, Bordage MC, Bray I, et al. LXCat: An open-access, web-based platform for data needed for modeling low temperature plasmas. *Plasma Process Polym* (2017) 14:1600098. doi:10.1002/PPAP.201600098

50. Carbone E, Graef W, Hagelaar G, Boer D, Hopkins MM, Stephens JC, et al. Data needs for modeling low-temperature non-equilibrium plasmas: The LXCat project, history, perspectives and a tutorial. *Atoms* (2021) 9:16. doi:10.3390/ATOMS9010016

51. Spyrou N, Held B, Peyrous R, Manassis C, Pignolet P. Gas temperature in a secondary streamer discharge: An approach to the electric wind. *J Phys D Appl Phys* (1992) 25:211–6. doi:10.1088/0022-3727/25/2/013

52. Komuro A, Matsuyuki S, Ando A. Simulation of pulsed positive streamer discharges in air at high temperatures. *Plasma Sourc Sci Technol* (2018) 27:105001. doi:10.1088/1361-6595/AADF5C

53. Zhang C, Cao W, Hung YC, Li B. Application of electrolyzed oxidizing water in production of radish sprouts to reduce natural microbiota. *Food Control* (2016) 67: 177–82. doi:10.1016/J.FOODCONT.2016.02.045

54. Wojtyla Ł, Lechowska K, Kubala S, Garnczarska M. Different modes of hydrogen peroxide action during seed germination. *Front Plant Sci* (2016) 7:66. doi:10.3389/fpls.2016.00066

55. Barba-Espin G, Diaz-Vivancos P, Clemente-Moreno MJ, Albacete A, Faize L, Faize M, et al. Interaction between hydrogen peroxide and plant hormones during germination and the early growth of pea seedlings. *Plant Cel Environ* (2010) 33:981–94. doi:10.1111/j.1365-3040.2010.02120.x

56. Sasaki K, Kishitani S, Abe F, Sato T. Promotion of seedling growth of seeds of rice (oryza sativa L. Cv. Hitomebore) by treatment with H 2 O 2 before sowing. *Plant Prod Sci* (2005) 8:509–14. doi:10.1626/pps.8.509

57. Xie Y, Ling T, Han Y, Liu K, Zheng Q, Huang L, et al. Carbon monoxide enhances salt tolerance by nitric oxide-mediated maintenance of ion homeostasis and up-regulation of antioxidant defence in wheat seedling roots. *Plant Cel Environ* (2008) 31:1864–81. doi:10.1111/J.1365-3040.2008.01888.X

58. Dekker J, Hargrove M. Weedy adaptation in Setaria spp. V. Effects of gaseous environment on giant foxtail (Setaria faberii) (Poaceae) seed germination. *Am J Bot* (2002) 89:410–6. doi:10.3732/AJB.89.3.410

59. Cao Z, Huang B, Wang Q, Xuan W, Ling T, Zhang B, et al. Involvement of carbon monoxide produced by heme oxygenase in ABA-induced stomatal closure in Vicia faba and its proposed signal transduction pathway. *Chin Sci Bull* (2007) 52:2365–73. doi:10.1007/s11434-007-0358-y

60. Cui W, Qi F, Zhang Y, Cao H, Zhang J, Wang R, et al. Methane-rich water induces cucumber adventitious rooting through heme oxygenase1/carbon monoxide and Ca2+ pathways. *Plant Cel Rep* (2015) 34:435–45. doi:10.1007/s00299-014-1723-3

61. Wang M, Liao W. Carbon monoxide as a signaling molecule in plants. *Front Plant Sci* (2016) 7:572. doi:10.3389/fpls.2016.00572

62. Fan L, Xia C, Zhu P, Lu Y, Wang H. Electrochemical CO2 reduction to high-concentration pure formic acid solutions in an all-solid-state reactor. *Nat Commun* (2020) 11:3633. doi:10.1038/S41467-020-17403-1

63. Hachiya T, Sakakibara H. Interactions between nitrate and ammonium in their uptake, allocation, assimilation, and signaling in plants. *J Exp Bot* (2017) 68:2501–12. doi:10.1093/jxb/erw449

64. Douat C, Escot Bocanegra P, Dozias S, Robert É, Motterlini R. Production of carbon monoxide from a He/CO2 plasma jet as a new strategy for therapeutic applications. *Plasma Process Polym* (2021) 18:2100069. doi:10.1002/PPAP.202100069